© 2016. Published by The Company of Biologists Ltd | Development (2016) 143, 2973-2982 doi:10.1242/dev.137513

RESEARCH ARTICLE

Apoptosis regulates endothelial cell number and capillary vessel diameter but not vessel regression during retinal angiogenesis

Emma C. Watson[1,2], Monica N. Koenig[1], Zoe L. Grant[1,2], Lachlan Whitehead[2,3], Evelyn Trounson[1], Grant Dewson[2,4] and Leigh Coultas[1,2,*]

ABSTRACT

The growth of hierarchical blood vessel networks occurs by angiogenesis. During this process, new vessel growth is accompanied by the removal of redundant vessel segments by selective vessel regression ('pruning') and a reduction in endothelial cell (EC) density in order to establish an efficient, hierarchical network. EC apoptosis has long been recognised for its association with angiogenesis, but its contribution to this process has remained unclear. We generated mice in which EC apoptosis was blocked by tissue-specific deletion of the apoptosis effector proteins BAK and BAX. Using the retina as a model, we found that apoptosis made a minor contribution to the efficiency of capillary regression around arteries where apoptosis was most concentrated, but was otherwise dispensable for vessel pruning. Instead, apoptosis was necessary for the removal of non-perfused vessel segments and the reduction in EC density that occurs during vessel maturation. In the absence of apoptosis, increased EC density resulted in an increase in the diameter of capillaries, but not arteries or veins. Our findings show that apoptosis does not influence the number of vessels generated during angiogenesis. Rather it removes non-perfused vessel segments and regulates EC number during vessel maturation, which has vessel-specific consequences for vessel diameter.

KEY WORDS: Angiogenesis, Apoptosis, Endothelial cell, Tissue remodelling, Hyaloid vessels

INTRODUCTION

Blood vessel networks consist of a hierarchical assembly of endothelial cell (EC)-lined tubes of varying identity and calibre, each necessary for the efficient distribution of blood throughout tissues. Whereas the first blood vessels to form emerge through the process of vasculogenesis (Coultas et al., 2005), their subsequent expansion and maturation into functional vascular networks occurs by angiogenesis: the coordinated proliferation, differentiation and migration of ECs and recruitment of perivascular support cells (Potente et al., 2011).

Apoptosis is a form of cell death responsible for the removal of excessive, damaged and otherwise redundant cells and tissues from the body (Czabotar et al., 2014). There are two distinct, but converging pathways that regulate apoptosis: the 'extrinsic', death receptor-mediated pathway and the 'intrinsic', BCL2-family mediated pathway. Both culminate in the activation of effector caspases (e.g. caspase 3), intracellular proteases that cause the proteolytic demolition of a cell. The extrinsic pathway involves the engagement of death receptors (e.g. Fas) by their cognate ligand (e.g. FasL), which triggers activation of caspase 8, and, in turn, activates downstream effector caspases (Strasser et al., 2009). In the intrinsic pathway, pro-survival members of the BCL2 family [BCL2, MCL1, BCLW (BCL2L2), BCL-XL (BCL2L1) and A1 (BCL2A1A)] prevent the activation of the structurally related pro-death proteins BAK (BAK1) and BAX. A third BCL2 sub-family, the so-called 'BH3-only' proteins [BIM (BCL2L11), BID, BAD, BIK, HRK, PUMA (BBC3) and NOXA (PMAIP1)], cause the activation of BAK and BAX through direct binding and by the inhibition of the pro-survival BCL2 proteins (Llambi et al., 2011). Activation of BAK and BAX leads to the permeabilisation of the mitochondrial outer membrane and release of apoptogenic factors such as cytochrome C (Wei et al., 2001). This in turn activates caspase 9 and subsequently the effector caspases. Apoptosis is responsible for tissue remodelling and regulating cell number in a range of tissues and organs during development (Fuchs and Steller, 2011) and much of this occurs through the intrinsic pathway, as shown by the combined loss of BAK and BAX (Lindsten et al., 2000). The intrinsic apoptosis pathway is essential for survival regulation in ECs: loss of the BH3-only protein BIM prevents EC apoptosis during normal and tumour-associated angiogenesis *in vivo* (Koenig et al., 2014; Naik et al., 2011; Wang et al., 2011), whereas EC-specific loss of the pro-survival BCL2 family protein MCL1 leads to ectopic EC apoptosis during angiogenesis *in vivo* (Watson et al., 2016).

Angiogenic blood vessel growth in the retina features many of the key processes that occur during hierarchical vessel network growth. Retina vessel angiogenesis in mice is attractive to study as it is amenable to imaging and is highly stereotypical, allowing detailed analysis of the angiogenesis process over time. Vascularisation of the mouse retina begins at birth, with the radial expansion of blood vessels from the optic nerve head at the centre of the retina towards the peripheral margin (Stahl et al., 2010). The growth of the vessel network requires extensive EC proliferation coupled with the emergence of new, blind-ended vessel sprouts that grow towards the avascular tissue then subsequently fuse by anastomosis to generate new, perfused vessels (Potente et al., 2011). This form of angiogenesis lays down a dense, uniform plexus of immature vessels that is remodelled through selective 'pruning' of individual vessel segments, converting the immature plexus into a refined, hierarchical network capable of efficient blood distribution (Korn and Augustin, 2015).

[1]Development and Cancer Division, The Walter and Eliza Hall Institute of Medical Research, 1G Royal Parade, Parkville, Victoria 3052, Australia. [2]University of Melbourne, Department of Medical Biology, 1G Royal Parade, Parkville, Victoria 3052, Australia. [3]Systems Biology and Personalised Medicine Division, The Walter and Eliza Hall Institute of Medical Research, 1G Royal Parade, Parkville, Victoria 3052, Australia. [4]Cell Signalling and Cell Death Division, The Walter and Eliza Hall Institute of Medical Research, 1G Royal Parade, Parkville, Victoria 3052, Australia.

*Author for correspondence (lcoultas@wehi.edu.au)

L.C., 0000-0001-6466-0890

Received 10 March 2016; Accepted 14 July 2016

Development (2016) 143, 2973-2982 doi:10.1242/dev.137513

Apoptosis is responsible for vessel regression under conditions of vessel network involution such as hyaloid vessel regression (Hahn et al., 2005; Koenig et al., 2014; Wang et al., 2011) and obliteration of retinal vessels in the oxygen-induced retinopathy model (Wang et al., 2011). Apoptosis is well-documented in retina angiogenesis, but reports differ as to its correlation with vessel pruning (Cheng et al., 2012; Hughes and Chan-Ling, 2000; Korn et al., 2014; Savant et al., 2015; Simonavicius et al., 2012), with as few as 5% of pruned vessels containing apoptotic ECs (Franco et al., 2015). Furthermore, apoptosis is rarely observed during vessel regression in zebrafish (Chen et al., 2012; Kochhan et al., 2013; Lenard et al., 2015), and is largely dispensable for the regression of those vessels in which it does occur (Kochhan et al., 2013). Live-imaging studies in zebrafish have recently shown that vessel regression occurs by EC migration, akin to 'anastomosis in reverse' (Chen et al., 2012; Lenard et al., 2015), and is triggered by local differences in blood flow between vessels (Chen et al., 2012; Kochhan et al., 2013; Lenard et al., 2015). A requirement for cell migration in blood vessel regression was also recently identified in the mouse retina (Franco et al., 2015). Thus, the contribution that apoptosis makes to the angiogenic process remains to be determined.

Here, we have genetically inactivated apoptosis in ECs to determine unequivocally the role of apoptosis during angiogenic vessel growth and maturation. Using a conditional knockout strategy, we generated mice lacking both of the apoptotic effector proteins BAK and BAX in ECs, which resulted in the complete suppression of EC apoptosis during angiogenesis. We found that apoptosis is required for removing non-perfused vessel segments that arise during vessel maturation and contributes to the establishment of optimal vessel diameter in capillaries, but not arteries or veins, by regulating EC number.

RESULTS

EC apoptosis is associated with regressing vessels and occurs through the intrinsic apoptotic pathway

Using activated caspase 3 staining as a marker for apoptosis, we quantified the distribution of apoptotic ECs across the vascular network of the retina. Consistent with previous reports (Simonavicius et al., 2012; Watson et al., 2016), we found that apoptosis was predominantly located around arteries at postnatal day (P) 6, with a limited amount around the veins and almost none in the sprouting region (Fig. 1A,B). This distribution is the opposite of EC proliferation at this time (Ehling et al., 2013). Of the apoptotic

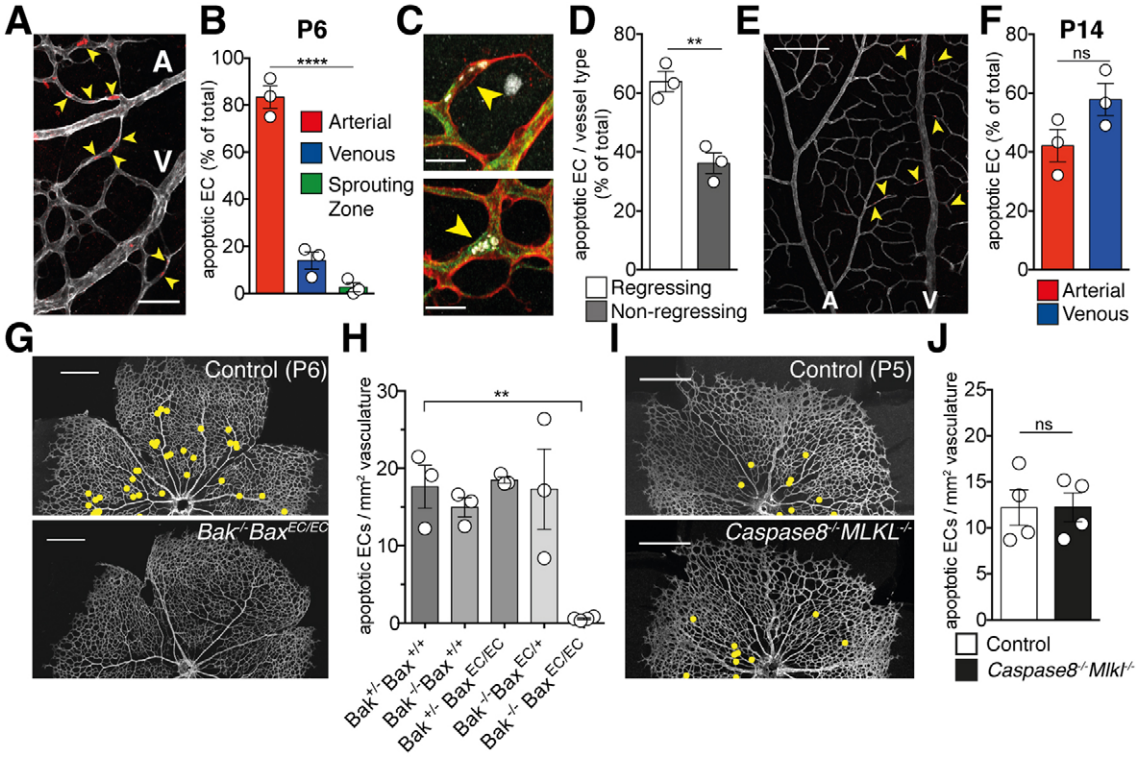

Fig. 1. EC apoptosis is associated with vessel regression and is dependent on BAK and BAX. (A) Representative image of apoptotic retina ECs at P6 stained for collagen IV (grey) and active caspase 3 (red). Yellow arrowheads indicate apoptotic ECs. (B) Location of apoptotic ECs by region in the retinal vasculature at P6 (n=3). Red bar, artery-proximal location; blue bar, vein-proximal location; green bar, sprouting zone. Data are presented as percentage of total apoptotic events. ****$P\leq0.0001$, one-way ANOVA. (C) Representative images of apoptotic ECs in regressing vessel (top panel) and non-regressing vessel (bottom panel). Yellow arrowheads indicate apoptotic EC. Red, collagen IV; green, PECAM1; grey, active caspase 3. (D) Quantification of EC apoptosis distribution in regressing (white bar) and non-regressing (grey bar) vessels (n=3) at P6. **$P\leq0.01$, two-tailed Student's t-test. (E) Representative image of apoptotic retina ECs at P14 stained for collagen IV (grey) and active caspase 3 (red). Yellow arrowheads indicate apoptotic ECs. (F) Distribution of apoptotic ECs by associated vessel type at P14 (n=3). ns, P>0.05, two-tailed Student's t-test. (G) Representative images from P6 control (top panel) and $Bak^{-/-}Bax^{EC/EC}$ (bottom panel) retinas stained for collagen IV (grey). Yellow dots indicate position of apoptotic (active caspase 3^+) ECs. (H) Quantification of apoptotic ECs of whole P6 retina relative to vessel area (collagen IV signal) from control ($Bak^{+/-}Bax^{+/+}$, n=3), $Bak^{-/-}Bax^{+/+}$ (n=3), $Bak^{+/-}Bax^{EC/EC}$ (n=3), $Bak^{-/-}Bax^{EC/+}$ (n=3) and $Bak^{-/-}Bax^{EC/EC}$ (n=4). **$P\leq0.01$, one-way ANOVA with Tukey's post-hoc multiple comparison test. (I) Representative images from P5 control ($Casp8^{+/-}Mlkl^{-/-}$, top panel) and $Casp8^{-/-}Mlkl^{-/-}$ (bottom panel) retinas stained for collagen IV (grey). Yellow dots indicate position of apoptotic (active caspase 3^+) ECs. (J) Quantification of apoptotic ECs of whole P5 retina relative to vessel area (collagen IV signal) from control (n=4) and $Casp8^{-/-}Mlkl^{-/-}$ (n=4). ns, P>0.05, two-tailed Student's t-test. All data are presented as mean±s.e.m. A, radial artery; V, radial vein. Scale bars: 50 µm (A); 20 µm (C); 200 µm (E); 500 µm (G,I).

Development (2016) 143, 2973-2982 doi:10.1242/dev.137513

ECs we observed, around two-thirds were found in regressing vessels (Fig. 1C,D). Active caspase 3^+ cells were also positive for terminal deoxynucleotidyl transferase dUTP nick end labelling (TUNEL), confirming they were apoptotic (Fig. S1A). We detected fewer apoptotic cells per P6 retina than did Franco et al. (2015), possibly owing to differences in mouse strain or quantification methods, such as our use of a monoclonal anti-active caspase 3 antibody. Substantial numbers of apoptotic ECs were still present at P14 (Fig. S1B), but, in contrast to P6, they were more evenly distributed, with preferential localisation around veins (Fig. 1E,F).

To investigate the role of apoptosis during angiogenesis, we generated mice in which apoptosis was blocked specifically in ECs. Although loss of the BH3-only protein BIM reduces EC apoptosis in the angiogenic retina (Koenig et al., 2014), it does not prevent EC apoptosis under all circumstances (Koenig et al., 2014; Watson et al., 2016), probably due to compensatory apoptosis initiation by other BH3-only proteins, as occurs in other cell types (Coultas et al., 2005). In order to overcome BH3-only protein redundancy and study angiogenesis in the complete absence of apoptosis, we generated mice in which ECs lacked both of the apoptosis effector proteins BAK and BAX. A conditional approach was required as the majority of *Bak/Bax* double knockouts are perinatal lethal (Lindsten et al., 2000). As such, we generated $Bak^{-/-}$ $Bax^{lox/lox}$ $Tie2\text{-}cre^{Tg/+}$ mice, which have ubiquitous loss of *Bak* and EC- and hematopoietic-specific loss of *Bax* owing to the *Tie2-cre* transgene (Kisanuki et al., 2001). These mice are hereafter referred to as $Bak^{-/-}Bax^{EC/EC}$. This approach was used as $Bak^{-/-}$ mice are healthy and fertile whereas $Bax^{-/-}$ males are infertile and have impaired apoptosis in a range of non-endothelial cell types in the developing retina (Hahn et al., 2003; Mosinger Ogilvie et al., 1998). Quantification of EC apoptosis across the whole retinal vasculature at P6 showed that although the presence of one functional allele of either *Bak* or *Bax* was sufficient to allow a normal level of apoptosis to occur, EC apoptosis was reduced by 97% in $Bak^{-/-}Bax^{EC/EC}$ mice (Fig. 1G,H).

To determine whether the extrinsic apoptosis pathway was somehow also required for EC apoptosis, we examined the retinas of $Casp8^{-/-}$ mice. In the absence of caspase 8, the alternative cell death pathway of necroptosis becomes activated causing embryonic lethality (Vince and Silke, 2016), which can be overcome by simultaneous deletion of the necroptosis effector MLKL (Etemadi et al., 2015). $Casp8^{-/-}Mlkl^{-/-}$ mice showed a small, non-significant reduction in EC apoptosis at P6 (Fig. S1C). This small difference was probably due to the mutants being runty rather than a specific defect in apoptosis (Fig. S1D) given no difference in EC apoptosis was observed at P5 when weights were similar (Fig. 1I,J). Taken together, these data show that apoptosis occurs predominantly, but not exclusively, in regressing vessels during angiogenesis and is triggered through the intrinsic apoptosis pathway.

Apoptosis is dispensable for vessel pruning during angiogenesis, but improves its efficiency

Given apoptosis was found predominantly in regressing vessels, we examined whether vessel regression was affected in $Bak^{-/-}Bax^{EC/EC}$ mice. We focused on the vessels around radial arteries at P6, as this was where the majority of apoptosis was found (Fig. 1B). Vessel density, measured by area, was not altered in the region immediately adjacent to arteries at P6 in $Bak^{-/-}Bax^{EC/EC}$ retinas compared with controls (Fig. 2A,B); however, a small but significant increase in the number of side branches connected to the radial artery was observed (Fig. 2A,C). This was in contrast to the plexus region, where no difference in vessel regression was observed (Fig. 2D). The increase in arterial side branches was nonetheless transient, as the number of side branches (and vessel density) was normal by P8 (Fig. 2E-G). These data indicate that EC apoptosis increases the efficiency of vessel pruning in high-flow capillaries, but is otherwise dispensable for vessel pruning.

We also observed clusters of ECs and vessel segments that were fully separated from the remaining circulation near arteries at P6 in $Bak^{-/-}Bax^{EC/EC}$ mice (observed in three out of four $Bak^{-/-}Bax^{EC/EC}$ mice) (Fig. 2H). In control mice, ECs in vessel segments that were regressing at both ends (an indication they were becoming isolated from the circulation) were apoptotic (Fig. 2H) and no persistent, isolated segments were observed in any control mice examined (n=12). These results suggest that apoptosis normally removes such non-perfused vessel segments.

Endothelial cell apoptosis does not limit the rate of new vessel production during angiogenesis

We next investigated whether apoptosis serves to limit the rate of angiogenesis. We examined the whole retinal vasculature of $Bak^{-/-}Bax^{EC/EC}$ mice at P6 and found that total vessel area and radial outgrowth were normal, indicating the rate of new vessel growth by sprouting angiogenesis was normal (Fig. 3A-C). Once the vascular network reaches the peripheral margin of the retina around P8, a second phase of sprouting occurs, extending perpendicular to the existing (superficial) vascular layer to form two new layers within in the retina (the 'intermediate' and 'deep' layers). We observed that secondary sprouts at P8 emerged closer to radial veins than arteries, and neither the number of secondary sprouts nor their distribution relative to the radial arteries and veins was changed in $Bak^{-/-}Bax^{EC/EC}$ mice (Fig. 3D,E). These results show that apoptosis does not limit the total amount of secondary sprouting or prevent it from occurring in the arterial region (Fig. 3E). When measured at P14, the amount of vasculature produced by secondary sprouting in the intermediate and deep vascular layers was also unchanged in $Bak^{-/-}$ $Bax^{EC/EC}$ mice compared with controls (Fig. 3F). Collectively, these results indicate that apoptosis does not restrict new vessel growth during angiogenesis.

Apoptosis regulates EC density during vessel network reorganisation and maturation

From P10 onwards, extensive vessel remodelling causes a reduction in vessel density through vessel pruning, reduced proliferation and a concurrent decline in EC density (Ehling et al., 2013). To investigate whether apoptosis contributed to this phase of angiogenesis, we quantified both vessel area and EC density in the retinal vasculature around arteries and veins of $Bak^{-/-}Bax^{EC/EC}$ mice from P8 through to 7 weeks of age (adulthood). We found that capillary vessel area around arteries and veins declined normally in $Bak^{-/-}Bax^{EC/EC}$ mice (Fig. 4A-C; Fig. S2A,B). Similar to observations at P8, EC clusters that were disconnected from the circulation were again observed in adult $Bak^{-/-}Bax^{EC/EC}$ retinas. These were clearly the product of vessel regression as some were still connected to patent vessels by thin sleeves of collagen IV (Fig. 4D). These aggregates were not found in control mice (n=10), again suggesting that apoptosis normally removes such non-perfused vessel segments.

To assess the effect of apoptosis on EC density, we quantified EC numbers in capillaries, arteries and veins using the nuclear marker FLI1 (Fig. 4A,B; Fig. S2A,B). In capillaries at P8, there was no difference in EC density in $Bak^{-/-}Bax^{EC/EC}$ mice compared with controls (Fig. S2C-E). Only the superficial layer was assessed as the deeper layers have not formed at this age. There was no detectable difference in the percentage of 5-ethynyl-2′-deoxyuridine $(EdU)^+$

Development (2016) 143, 2973-2982 doi:10.1242/dev.137513

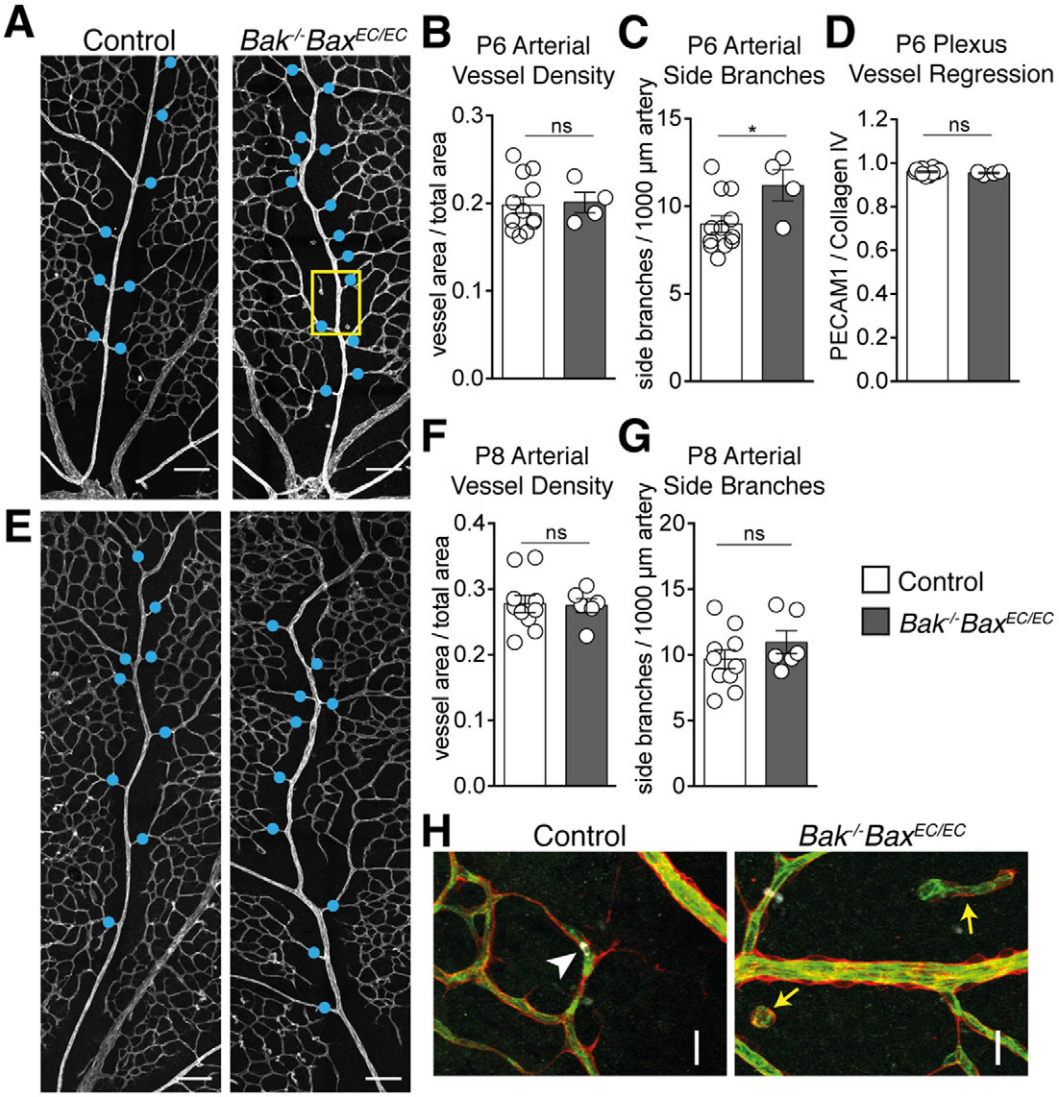

Fig. 2. Apoptosis is dispensable for vessel pruning during angiogenesis but improves its efficiency in high-flow capillaries. (A,E) Representative images of arterial regions from control (left panel) and $Bak^{-/-}Bax^{EC/EC}$ (right panel) retinas stained for PECAM1 at P6 (A) and P8 (E). Blue dots indicate artery side branches. Box indicates area magnified in H. (B,C) Quantification of vessel density around a major (radial) artery (B) and side branches per 1000 µm of radial artery length (C) for control (white bars, n=12) and $Bak^{-/-}Bax^{EC/EC}$ (grey bars, n=4) at P6. (D) Quantification of vessel regression in plexus regions of control (white bar, n=12) and $Bak^{-/-}Bax^{EC/EC}$ (grey bar, n=4) mice at P6, determined by the ratio of PECAM1-positive vessel segments to collagen IV-positive vessel segments. (F,G) Quantification of vessel density around a major (radial) artery (F) and side branches per 1000 µm of radial artery length (G) for control (white bars, n=10) and $Bak^{-/-}Bax^{EC/EC}$ (grey bars, n=6) at P8. (H) Representative images of disconnected vessel segments stained for collagen IV (red), PECAM1 (green) and active caspase 3 (grey) at P6 in control and $Bak^{-/-}Bax^{EC/EC}$ retinas. White arrowhead indicates disconnected vessel segment with apoptotic EC. Yellow arrows indicate disconnected vessel segments with no apoptotic ECs. All data are presented as mean±s.e.m. ns, P>0.05; *P≤0.05, two-tailed Student's t-test. Scale bars: 100 µm (A,E); 20 µm (H).

ECs between control and $Bak^{-/-}Bax^{EC/EC}$ mice, which might have been expected to compensate for the additional cells expected in the absence of apoptosis (Fig. S2F). After P8, control mice showed the expected decline in overall EC density. We found that capillary EC density around arteries declined rapidly between P8 and P14 in control mice, whereas this did not occur in $Bak^{-/-}Bax^{EC/EC}$ mice (Fig. 4E). The decline in EC density in venous capillaries of control mice occurred more gradually, but remained unaltered in $Bak^{-/-}Bax^{EC/EC}$ mice, with significantly more ECs present by adulthood (Fig. 4E). Overall, total capillary EC density remained unchanged between P8 and adulthood in $Bak^{-/-}Bax^{EC/EC}$ mice (Fig. 4F). This increase in EC density in capillaries was due to an increase in absolute EC number, which was more striking in venous capillaries (Fig. 4G). In the radial artery and radial vein, EC number and density was also increased (Fig. 4H,I). These results demonstrate that the reduction in EC density that occurs during vessel maturation is dependent on apoptosis.

Although the absence of apoptosis did not prevent the age-related reduction in vessel area by adulthood, we did notice a subtle, but non-significant (11.6%) increase in vessel area in the venous region of adult $Bak^{-/-}Bax^{EC/EC}$ mice (Fig. 4C). This was not due to increased vessel number or vessel length as total capillary length in this region was normal (Fig. 5A). Instead, the increase in vessel area was due to an increase in capillary width, with a 10-16% increase in capillary width depending on the layer (Fig. 5B,C). Quantification of the average vessel width using 3D surface-rendered images showed an overall 11% increase in venous capillary width in $Bak^{-/-}Bax^{EC/EC}$ mice (Fig. 5D,E). A similar trend towards increased vessel

Development (2016) 143, 2973-2982 doi:10.1242/dev.137513

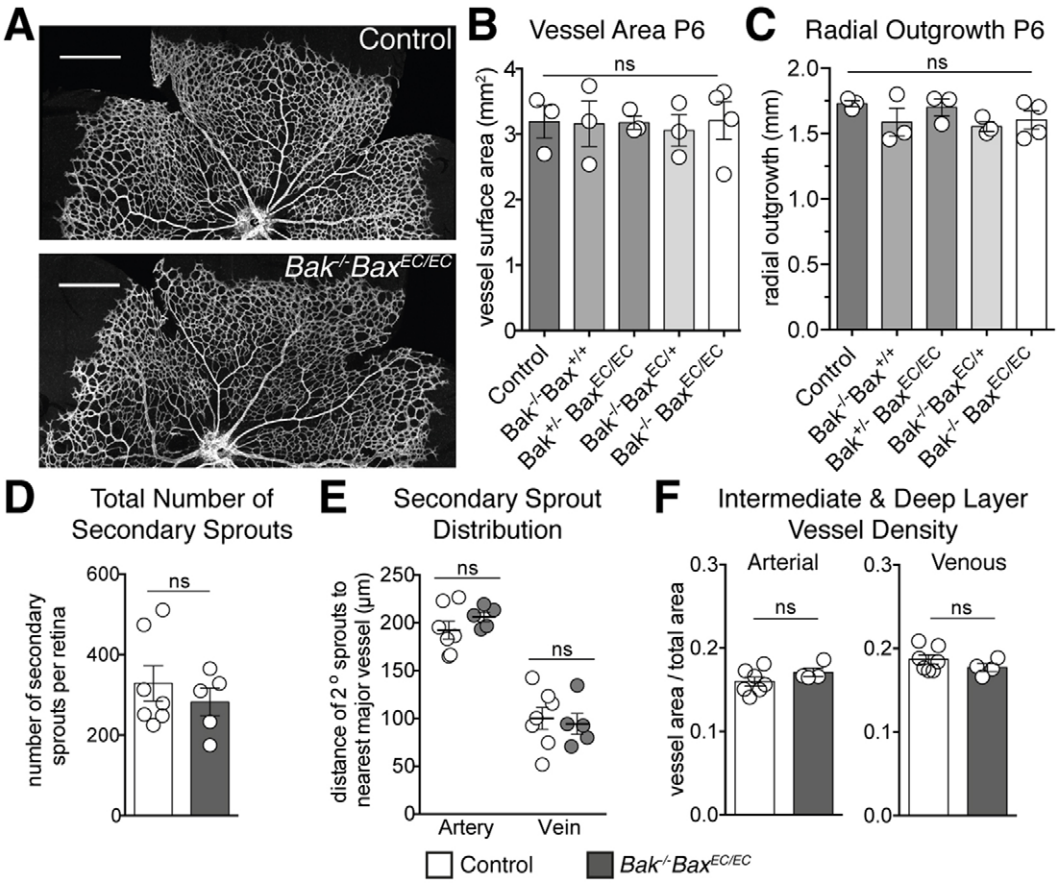

Fig. 3. EC apoptosis does not limit the rate of angiogenic vessel production. (A) Representative images of collagen IV-stained P6 control (top panel) and $Bak^{-/-}Bax^{EC/EC}$ (bottom panel) vasculature. Scale bars: 500 µm. (B,C) Quantification of total vessel surface area (B) and radial outgrowth (C), quantified using collagen IV signal from control ($Bak^{+/-}Bax^{+/+}$, n=3), $Bak^{-/-}Bax^{+/+}$ (n=3), $Bak^{+/-}Bax^{EC/EC}$ (n=3), $Bak^{-/-}Bax^{EC/+}$ (n=3) and $Bak^{-/-}Bax^{EC/EC}$ (n=4). ns, P>0.05, one-way ANOVA. (D) Quantification of secondary sprouts per retina at P8 for control (white bar, n=7) and $Bak^{-/-}Bax^{EC/EC}$ (grey bar, n=5). (E) Distribution of secondary sprouts at P8 for control (white circles, n=7) and $Bak^{-/-}Bax^{EC/EC}$ (grey circles, n=5). (F) Vessel density of intermediate and deep layers of vasculature combined at P14. Arterial region (left panel) and venous region (right panel) for control (white bars, n=7) and $Bak^{-/-}Bax^{EC/EC}$ (grey bars, n=4). ns, P>0.05, two-tailed Student's t-test. All data are presented as mean±s.e.m.

width was also found in some arterial capillaries but did not reach significance, probably because the increase in EC number was not as pronounced as it was in venous capillaries (Fig. 4G; Fig. S3). In contrast to capillaries, there was no increase in vessel width in the radial artery or vein despite increased EC number in these vessels (Fig. 5F). Together, these data show that apoptosis is not required to regulate vessel density during the maturation of blood vessels, but it is required to reduce EC number per vessel, which in turn can influence capillary diameter, particularly around veins.

Hyaloid vessel regression in $Bak^{-/-}Bax^{EC/EC}$ mutants

Hyaloid vessels undergo postnatal regression that is dependent on apoptosis. Consistent with previous reports (Hahn et al., 2005), we observed a significant reduction in the number of hyaloid vessel segments undergoing apoptotic regression in P5 $Bak^{-/-}Bax^{EC/EC}$ mice versus controls (Fig. 6A,B). Apoptotic vessel regression was completely absent or nearly absent in three out of five mutants, whereas one animal showed normal hyaloid apoptosis, possibly due to cre inefficiency, which we occasionally observe with *Tie2-cre* (Watson et al., 2016). At 4 weeks of age, hyaloid vessels had fully regressed in control mice. By contrast, $Bak^{-/-}Bax^{EC/EC}$ mice at this age contained an extensive network of hyaloid vasculature, and perfusion labelling showed that most, but not all, was functional (Fig. 6C). Notably, we observed large numbers of non-perfused EC clusters among the persistent hyaloids that were similar to those observed in the mutant retina (Fig. 6D,E). These clusters were often connected to a sleeve of collagen IV, suggesting they arose from regressing vessels (Fig. 6D,E). Consistent with this, we observed isolated clusters of ECs forming within regressing vessel segments early on in hyaloid regression at P5. These clusters were present in both control and $Bak^{-/-}Bax^{EC/EC}$ mice, the difference being they were apoptotic in controls but not in the mutants (Fig. 6F). These results strongly suggest that isolated EC clusters arise during vessel regression and are normally removed by apoptosis.

Hyaloid vessel regression was not completely prevented in $Bak^{-/-}Bax^{EC/EC}$ mutants, raising the possibility that an apoptosis-independent mechanism might contribute to hyaloid regression. Consistent with this, we observed numerous TUNEL-negative regressing vessels in wild-type mice. Among these were ECs with front-rear polarity indicative of migration towards neighbouring vessels based on Golgi marker staining (Fig. 6G). This suggests that vessel regression via cell migration also contributes to hyaloid regression, similar to that which occurs in the retina (Franco et al., 2015).

DISCUSSION

The association between EC death and vessel regression during angiogenic remodelling in the retina has been made since the 1960s

Development (2016) 143, 2973-2982 doi:10.1242/dev.137513

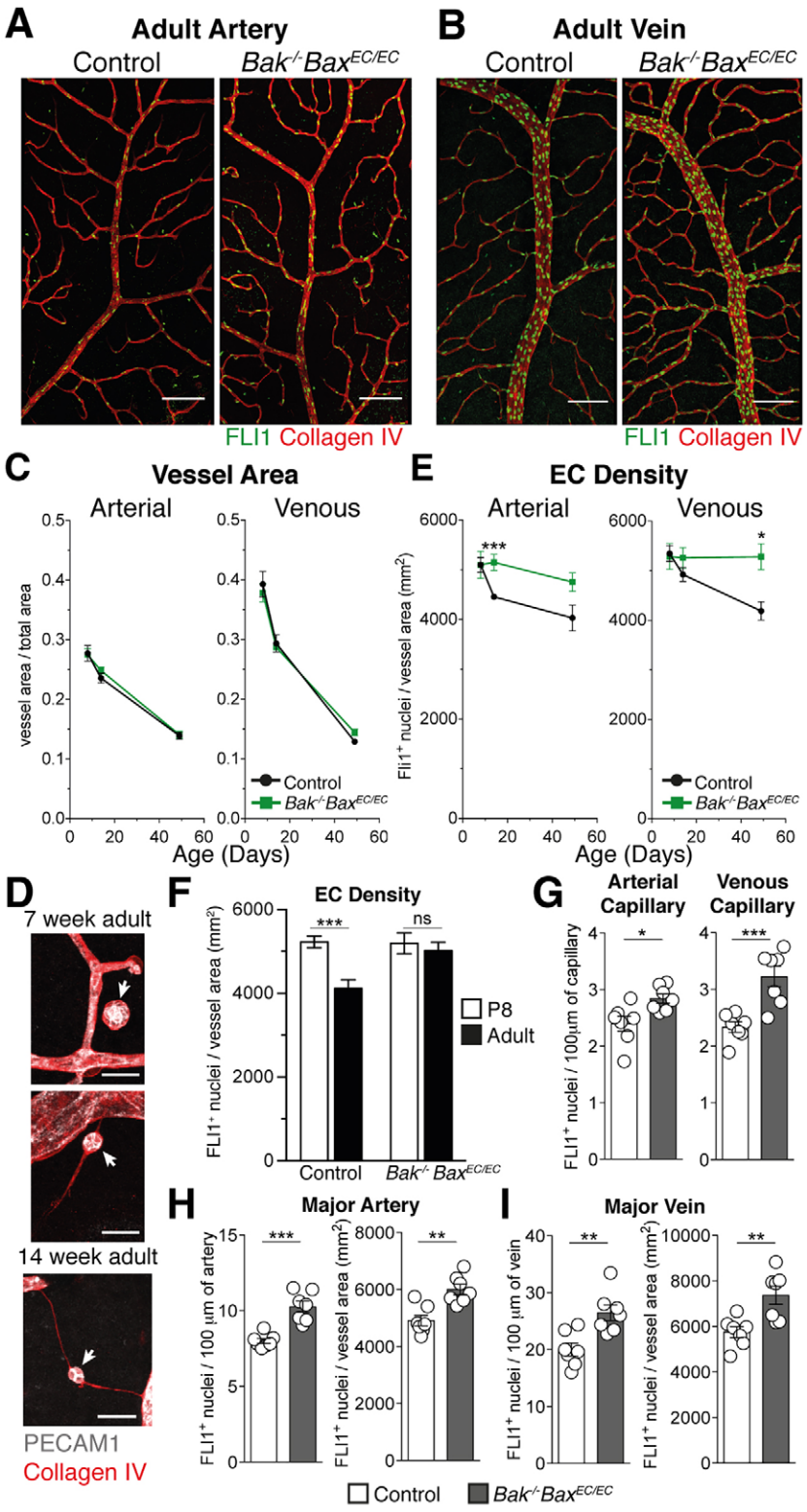

Fig. 4. Apoptosis regulates EC density during maturation. (A,B) Representative images of EC density in adult arterial region (A) and adult venous region (B) in control (left panel) and $Bak^{-/-}Bax^{EC/EC}$ (right panel) retinas stained for collagen IV (red) and FLI1 (green). Scale bars: 100 µm. (C) Quantification of capillary vessel area in arterial region (left panel) and venous region (right panel) with age (days). (D) Representative images of EC aggregates disconnected from the circulation in adult retinas (white arrows) stained for collagen IV (red), PECAM1 (grey) at 7 weeks (top panels) and 14 weeks (bottom panel) of age. Scale bars: 20 µm. (E) Quantification of capillary EC density in arterial region (left panel) and venous region (right panel) with age (days). (F) Comparison of EC density between P8 (white bars) and adults (black bars) in control and $Bak^{-/-}Bax^{EC/EC}$ mice for combined arterial and venous regions. (G) Quantification of adult capillary EC number in arterial region (left panel) and venous region (right panel). (H) Quantification of adult major (radial) artery EC number (left panel) and EC density (right panel). (I) Quantification of adult major (radial) vein EC number (left panel) and EC density (right panel) for control (white bars) and $Bak^{-/-}Bax^{EC/EC}$ (grey bars). For all panels, data were collected at P8 (control, n=10; $Bak^{-/-}Bax^{EC/EC}$, n=6), P14 (control, n=7; $Bak^{-/-}Bax^{EC/EC}$, n=4) and 7 weeks (control, n=7; $Bak^{-/-}Bax^{EC/EC}$, n=7). All data are presented as mean±s.e.m. ns, P>0.05; *P<0.05; **P≤0.01; ***P≤0.001, two-tailed Student's t-test with Holm–Sidak correction for multiple testing in C, E and F.

(Ashton, 1966), yet formal investigation of its functional role in angiogenesis has been lacking. Studies in the pupillary membrane have shown that EC apoptosis can initiate blood vessel regression as dying ECs can occlude vessels, leading to flow stasis and subsequent vessel regression (Meeson et al., 1996). Our finding that vessel regression in the retina is not prevented in the absence of apoptosis argues that this model does not apply in the case of controlled, angiogenic vessel pruning. This is consistent with recent evidence showing that vessel pruning occurs by cell migration in response to local differences in blood flow between vessels (Chen et al., 2012; Franco et al., 2015; Kochhan et al., 2013; Lenard et al., 2015). Nonetheless, we found that blood vessel regression in arterial side branches was delayed in the absence of apoptosis, indicating that it is required to make the process more efficient. Apoptosis

Development (2016) 143, 2973-2982 doi:10.1242/dev.137513

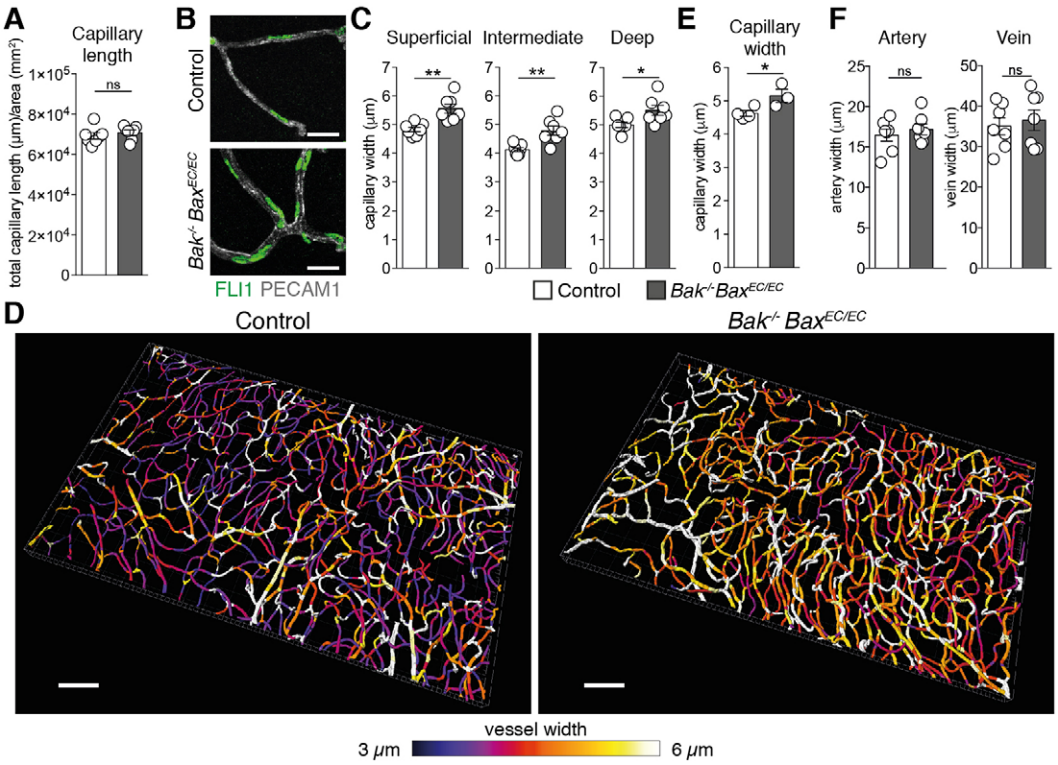

Fig. 5. Capillary vessel width is increased in regions of increased EC density. (A) Quantification of total capillary length in venous region of adult control (white bar, *n*=7) and $Bak^{-/-}Bax^{EC/EC}$ (grey bar, *n*=7) mice. (B) Representative images of venous capillaries in control (top panel) and $Bak^{-/-}Bax^{EC/EC}$ (bottom panel) adult retinas stained for PECAM1 (grey) and FLI1 (green). Scale bars: 20 µm. (C) Quantification of adult venous capillary width in the superficial, intermediate and deep layers for control (white bars, *n*=7) and $Bak^{-/-}Bax^{EC/EC}$ (grey bars, *n*=7). (D) Representative 3D surface-rendered images of PECAM1 signal in capillary vasculature of adult retina venous region. Vessel segments are colour coded by vessel width. Scale bars: 100 µm. (E) Quantification of venous region capillary width from 3D surface-rendered PECAM1 images for control (white bar, *n*=4) and $Bak^{-/-}Bax^{EC/EC}$ (grey bar, *n*=3). (F) Quantification of adult major (radial) artery (left panel) and vein (right panel) widths for control (white bars, *n*=7) and $Bak^{-/-}Bax^{EC/EC}$ (grey bars, *n*=7). All data are presented as mean±s.e.m. ns, $P>0.05$; *$P\leq0.05$; **$P\leq0.01$, two-tailed Student's *t*-test, with Holm–Sidak multiple test correction for C.

might enhance vessel regression by reducing the number of cells that need to migrate and integrate into neighbouring vessels, accelerating the exit of all cells from the regressing vessel. Alternatively, in epithelial monolayers, apoptotic cells exert forces on their neighbouring cells, inducing autonomous and non-cell autonomous shape changes in those cells (Kuipers et al., 2014). It is possible that similar forces are generated by dying ECs and these may act to enhance the cell shape changes necessary for cellular rearrangement during vessel regression. As no defect in vessel pruning was observed other than in arterial side-branches, this function for apoptosis might be peculiar to high-flow capillaries and possibly indicative of a specific type of vessel regression.

We found that EC apoptosis was predominantly located in regressing vessels during angiogenesis and several studies have previously shown that levels of EC apoptosis during retina angiogenesis directly correlate with levels of vessel regression (Cheng et al., 2012; Korn et al., 2014; Savant et al., 2015; Simonavicius et al., 2012). Despite this, our genetic approach of inactivating EC apoptosis shows that it is not causative of vessel regression, consistent with recent findings that only 5% of regressing vessels in the retina contain apoptotic ECs (Franco et al., 2015). Non-canonical Wnt signalling has been variously suggested to control vessel regression by regulating EC apoptosis (Korn et al., 2014; Scholz et al., 2016) or EC sensitivity to blood flow-induced cell migration (Franco et al., 2016). Our data argue against a role for apoptosis promoting vessel regression during angiogenesis. Furthermore, mice with EC-specific loss of the pro-survival protein MCL1 exhibited a far greater increase in apoptosis than that reported for mice lacking non-canonical Wnt, but did not show an increase in vessel regression (Watson et al., 2016). These findings would argue against a role for apoptosis in promoting vessel regression, even when ectopically activated. Instead, changes within the regressing vessel such as cessation of blood flow (as occurs in 'type 1' vessel regression; Lenard et al., 2015), probably trigger apoptosis in a subset of ECs that are unable to migrate to the 'protective' environment of a perfused vessel (Franco et al., 2015). This interpretation is supported by our finding that apoptosis removes ECs from non-perfused vessels in the retina and hyaloid networks.

We found that apoptosis was responsible for the reduction in EC density that occurs in the angiogenic vasculature as it remodels into a mature network. However, EC density was not affected early in angiogenesis at P8. It is impossible to estimate the exact number of ECs that die by apoptosis during the early stages of retina angiogenesis, making it impossible to predict accurately the number of supernumerary cells expected in its absence and, therefore, whether we would expect to detect an increase in the mutants by P8. Reduced proliferation might compensate for reduced apoptosis to maintain normal cell number, but we found this was unchanged in the mutants. However, even a small decrease in proliferation can have a substantial effect on cell number over time and it remains possible that the proliferation detection method we used was not sufficiently sensitive to reveal changes in proliferation rates that might be compensating for the lack of apoptosis.

Development (2016) 143, 2973-2982 doi:10.1242/dev.137513

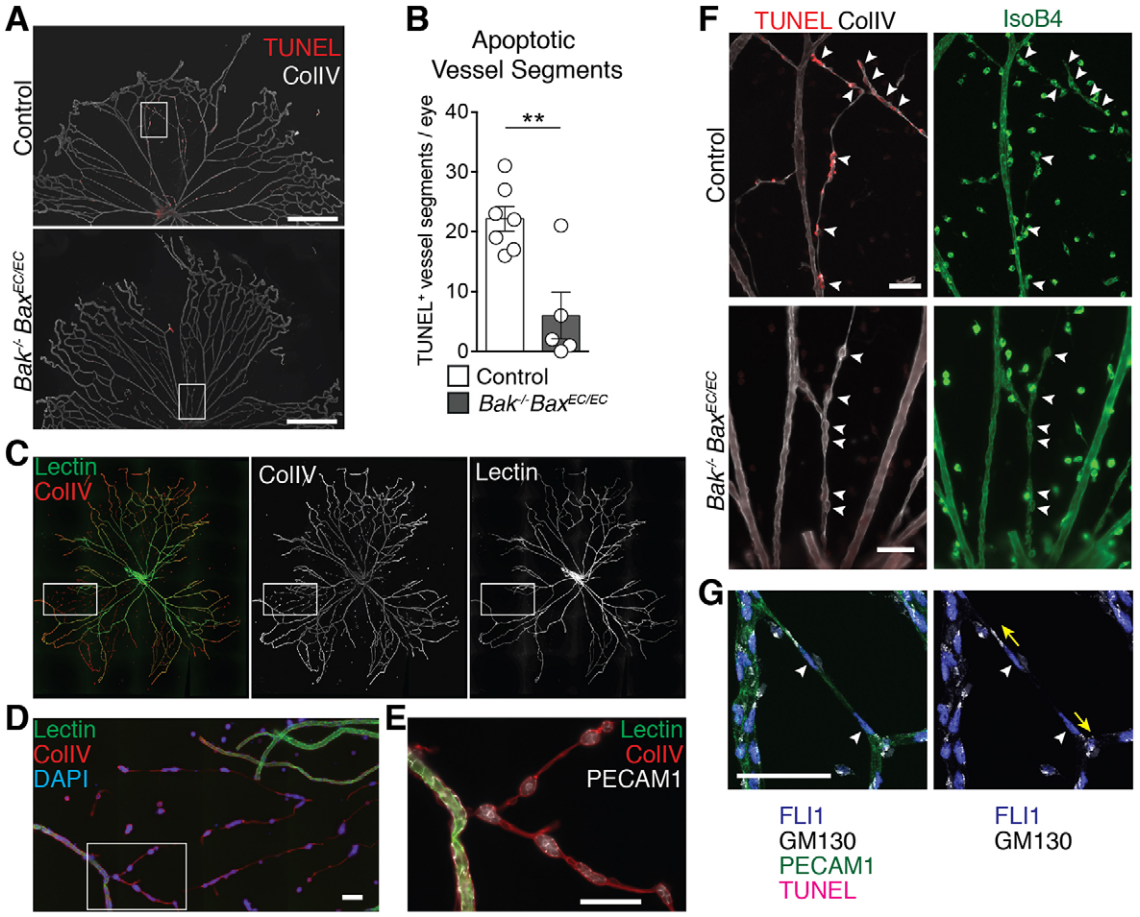

Fig. 6. Hyaloid regression is disrupted in the absence of EC apoptosis. (A) Representative images of hyaloid vessels at P5 from control and $Bak^{-/-}Bax^{EC/EC}$ littermates stained for TUNEL (red) and collagen IV (grey). Boxes indicate regions shown in F. (B) Quantification of TUNEL$^+$ vessel segments in P5 control (n=7) and $Bak^{-/-}Bax^{EC/EC}$ (n=5) littermates. Data are mean±s.e.m. **P<0.01, two-tailed Student's t-test. (C) Representative image of hyaloid vessel from a 4-week-old $Bak^{-/-}Bax^{EC/EC}$ mouse perfused with *L. esculentum* lectin (green) and stained for collagen IV (red) (n=3). Box indicates region shown in D. (D) Higher magnification of the boxed region in C including DAPI signal (blue). Box indicates region shown in E. (E) Higher magnification of the boxed region in D including PECAM1 signal (grey). (F) Higher magnifications of the boxed regions in A including isolectin B4 signal (green). White arrowheads indicate isolated, isolectin B4$^+$ EC clusters. (G) Confocal image of regressing hyaloid vessel from a wild-type animal stained with FLI1 (blue), GM130 (grey), PECAM1 (green) and TUNEL (magenta). White arrowheads indicate migrating ECs, yellow arrows indicate direction of migration based on Golgi location relative to the nucleus. Scale bars: 500 µm (A); 50 µm (D,E,F,G).

Our results show that increased EC number in adults was associated with increased diameter in capillaries, principally those near veins. Mice in which ECs lack *Rbpjk* (*Rbpj*) or *Foxo1* also have increased EC number and an increase in retinal vessel diameter (Ehling et al., 2013; Wilhelm et al., 2016). Notably, however, both these mutants show an increase in vein diameter, which we did not observe. In the case of *Rbpjk* mutants, the difference is likely to be due to increased EC size as well as number (Ehling et al., 2013). Although EC size was not reported for the *Foxo1* mutants, it is at least possible it is increased given their upregulation of MYC (Wilhelm et al., 2016), a known positive regulator of cell growth (Dang, 2013). The absence of increased artery or vein diameter in the $Bak^{-/-}Bax^{EC/EC}$ mice despite increased cell number suggests there must be strong feedback mechanisms in place to maintain a preferred diameter in these vessels, regardless of cell number. Our findings suggest these mechanisms are not as strong in capillaries. One possible explanation is related to perivascular support cell coverage. In adult retinas, arteries and veins are both covered in smooth muscle (Ehling et al., 2013), and these may be more effective at regulating vessel diameter than the pericytes covering the capillaries. Retinal vasculature is subject to metabolic regulation (Pournaras et al., 2008), and although the smooth muscle layer around retinal veins is thinner and less organised than arteries, there is evidence that it is capable of vasoconstriction (Yu et al., 2016). The functional consequence of increased EC density and capillary diameter on retinal vascular function and metabolic regulation in particular deserves further investigation.

Previous studies have suggested that Fas/FasL-driven EC apoptosis is responsible for vessel pruning in the angiogenic retina vasculature (Ishida et al., 2003). However, retina vessel development was reportedly normal in $FasL^{gld}$ mice (Davies et al., 2003). Our data using caspase 8-deficient mice strongly suggest that death receptor-mediated apoptosis is not required for EC apoptosis during angiogenesis and excludes the possibility of redundancy from other death receptors in the absence of Fas.

Apoptotic capillary regression in pupillary membrane has been proposed to involve two stages of EC apoptosis (Meeson et al., 1996). The first, dependent on macrophages, causes stenosis that triggers a second, synchronous wave of apoptosis in the remaining ECs as they are simultaneously deprived of the protective effects of laminar blood flow. The requirement for macrophages and the presence of synchronous apoptosis in hyaloid vessels suggests this

Development (2016) 143, 2973-2982 doi:10.1242/dev.137513

model is also responsible for their regression (Lobov et al., 2005). The presence of functional hyaloid vessels in our $Bak^{-/-}Bax^{EC/EC}$ mice is consistent with EC apoptosis being an initial trigger for vessel stenosis and the subsequent regression of hyaloid vessels. However, some hyaloid regression still occurred in the $Bak^{-/-}Bax^{EC/EC}$ mice. Although this may have been due to the residual apoptosis present in the mutants (probably due to imperfect cre efficiency), it also suggests that additional mechanisms may provide the regression trigger in certain hyaloid vessels. Indeed, we found evidence for polarised cell migration during hyaloid vessel regression, similar to that which occurs in the retina (Franco et al., 2015). Regardless of the initial trigger, our data clearly show that apoptosis was responsible for the second, synchronous wave of apoptosis that clears ECs from the non-perfused vessels. In the absence of apoptosis, these cells formed long-lived aggregates of EC. The similarity of retina EC aggregates to those in the hyaloids suggests they also arise through vessel regression. Defective retinal vascularisation phenotypes are often associated with persistent hyaloid vasculature (Saint-Geniez and D'Amore, 2004). In these cases, the presence of persistent hyaloids has been attributed to defects in the retinal vasculature, probably through increased retina hypoxia and a subsequent increase in VEGFA expression (Xu et al., 2004). Increased VEGFA levels or perturbation of VEGFA isoform expression are associated with persistent hyaloid vessels (Kurihara et al., 2010; Rao et al., 2013; Stalmans et al., 2002). In some cases, however, it has been suggested that persistent hyaloid vessels are causal for accompanying retinal vascular defects (Kurihara et al., 2010). Our data show that the presence of hyaloid vasculature by itself does not disrupt retinal vascular development. This would suggest either that retinal vascular defects are more likely to cause persistent hyaloids, or that certain mutations affect pathways common to both retinal angiogenesis and hyaloid regression.

Our results show that during angiogenic vessel remodelling, apoptosis is a consequence of vessel regression, not a cause, and that its principal role is to regulate EC number and remove non-perfused vessel segments. Understanding mechanisms of cell migration will provide greater insight into vessel remodelling and capillary density during angiogenesis, whereas understanding apoptosis control will shed new light on how EC density is determined and possibly vessel calibre and function.

MATERIALS AND METHODS

Mice

All experiments involving animals were performed with procedures approved by the Walter and Eliza Hall Institute of Medical Research Animal Ethics Committee. For lectin perfusion, 4-week-old mice were anaesthetised with Xylazil-20 (20 mg/kg) (Troy laboratories Pty Ltd) and Ketamine (100 mg/kg) (Hospira Australia Pty Ltd) via intraperitoneal injection, then injected intravenously with 100 µg of DyLight488-conjugated *Lycopersicon esculentum* (tomato) lectin (Vector Laboratories, DL-1174) and allowed to circulate for 5 min prior to perfusion fixation with 4% paraformaldehyde via the left ventricle. See supplementary Materials and Methods for strain details.

Immunohistochemical staining

Eyes were fixed in 4% paraformaldehyde before dissecting and staining retinas in PBS with 1% Triton X-100 and 2% donkey serum. See supplementary Materials and Methods for antibody details. For proliferation assessment, 100 µg EdU was administered to P6 pups by intraperitoneal injection and labelled for 2 h. Click-iT EdU Alexa Fluor 647 (Thermo Fisher, C10340) was performed according to manufacturer's instructions. For combined active caspase 3/TUNEL staining, retinas were fixed and dissected as above, washed, then incubated in trypsin-EDTA (Invitrogen, 59430C) until the vascular layer dissociated from the retina. Retinal vessels were incubated in reaction buffer containing 0.5 U/µl terminal deoxynucleotidyl transferase (Promega), 1 mM $CoCl_2$ and 0.15 nM biotinylated-dUTP (Roche). $TUNEL^+$ cells were detected with streptavidin-Alexa Fluor 488 at 1/400 (Jackson ImmunoResearch, 016-540-084, lot #106784). For hyaloid staining, eyes were fixed as described above then injected with 5% gelatin in PBS and allowed to set overnight at 4°C. Gelatin plugs were dissected and flat-mounted on polysine slides (Thermo Scientific) prior to staining with antibodies as per whole-mount retina staining or TUNEL using the ApopTag Red *in situ* apoptosis detection kit as per the manufacturer's instructions (Millipore) with the exception that incubations were performed at room temperature. Biotinylated-isolectin B4 staining of hyaloids (20 µg/ml, Vector Labs B-1105, lot #X0831) was performed in Hank's balanced salt solution containing Ca^{2+} and Mg^{2+}, 1% Triton X-100 and 2% normal donkey serum and was detected with streptavidin-Alexa Fluor 488 at 1/400 (Jackson ImmunoResearch, 016-540-084, lot #106784). All samples were mounted in ProLong Gold containing DAPI (Invitrogen).

Image analysis

All retina imaging was performed using a Leica SP8 confocal microscope with either 20×/0.75 NA objective or 40×/1.30 NA using Leica Application Suite software. Retina image analysis methods are detailed in supplementary Materials and Methods. Hyaloid samples were imaged by wide-field microscopy (unless indicated) using a Zeiss Axiovert 200M (Zeiss) equipped with a Zeiss MRm Axiocam camera, and 10×/0.45 NA or 40×/1.4 NA Plan-Apochromat objectives. A 0.63× C-mount was used for some images. Image analysis was performed in the FIJI distribution of ImageJ software (Schindelin et al., 2012).

Statistics

Statistical analysis was performed using one-way analysis of variance test with Tukey's multiple comparison test where multiple groups were compared. Two-tailed Student's *t*-test was used when two groups were compared, with Holm–Sidak correction applied when multiple tests were applied to a dataset.

Acknowledgements

The authors thank Mark Scott and Kelly Rogers (Walter and Eliza Hall Institute of Medical Research) for expert imaging assistance; Douglas Green (St Jude Children's Research Hospital, Memphis) for *Bax* conditional allele mice; Masashi Yanagisawa (University of Texas Southwestern Medical Center) for *Tie2-cre* mice; Razqallah Hakem (University of Toronto) for *caspase* $8^{-/-}$ mice; Warren Alexander (Walter and Eliza Hall Institute of Medical Research) for $Mlkl^{-/-}$ and double knockout $Caspase8^{-/-}Mlkl^{-/-}$ mice; Glenna-Faye Dabrowski, Melissa Pritchard, Jaclyn Gilbert, Emma Lanera and Dannielle Cooper for expert animal care; Andreas Strasser (Walter and Eliza Hall Institute of Medical Research), Robert C. A. Symons (Royal Melbourne Hospital), Anne K. Voss (Walter and Eliza Hall Institute of Medical Research) and members of the Development and Cancer Division (Walter and Eliza Hall Institute of Medical Research) for informative discussion.

Competing interests

The authors declare no competing or financial interests.

Author contributions

E.C.W. performed research, analysed data and wrote the paper. M.N.K., Z.L.G. and E.T. performed research. L.W. generated analytical tools and analysed data. G.D. analysed data. L.C. designed research, analysed data and wrote the paper.

Funding

This work was made possible through Victorian State Government Operational Infrastructure Support and Australian Government NHMRC IRIISS. This work was supported by the National Health and Medical Research Council, Australia [Project Grant: 1010638 to L.C.]; the Australian Research Council [Future Fellowships: 110100891 to L.C., 100100791 to G.D.]; and the L.E.W Carty Charitable Fund.

Supplementary information

Supplementary information available online at
http://dev.biologists.org/lookup/doi/10.1242/dev.137513.supplemental

Development (2016) 143, 2973-2982 doi:10.1242/dev.137513

References

Ashton, N. (1966). Oxygen and the growth and development of retinal vessels. In vivo and in vitro studies. The XX Francis I. Proctor Lecture. *Am. J. Ophthalmol.* **62**, 412-435.

Chen, Q., Jiang, L., Li, C., Hu, D., Bu, J.-w., Cai, D. and Du, J.-l. (2012). Haemodynamics-driven developmental pruning of brain vasculature in zebrafish. *PLoS Biol.* **10**, e1001374.

Cheng, C., Haasdijk, R., Tempel, D., van de Kamp, E. H. M., Herpers, R., Bos, F., Den Dekker, W. K., Blonden, L. A. J., de Jong, R., Burgisser, P. E. et al. (2012). Endothelial cell-specific FGD5 involvement in vascular pruning defines neovessel fate in mice. *Circulation* **125**, 3142-3159.

Coultas, L., Chawengsaksophak, K. and Rossant, J. (2005). Endothelial cells and VEGF in vascular development. *Nature* **438**, 937-945.

Czabotar, P. E., Lessene, G., Strasser, A. and Adams, J. M. (2014). Control of apoptosis by the BCL-2 protein family: implications for physiology and therapy. *Nat. Rev. Mol. Cell Biol.* **15**, 49-63.

Dang, C. V. (2013). MYC, metabolism, cell growth, and tumorigenesis. *Cold Spring Harb. Perspect. Med.* **3**, a014217

Davies, M. H., Eubanks, J. P. and Powers, M. R. (2003). Increased retinal neovascularization in Fas ligand–deficient mice. *Invest. Ophthalmol. Vis. Sci.* **44**, 3202-3210.

Ehling, M., Adams, S., Benedito, R. and Adams, R. H. (2013). Notch controls retinal blood vessel maturation and quiescence. *Development* **140**, 3051-3061.

Etemadi, N., Chopin, M., Anderton, H., Tanzer, M. C., Rickard, J. A., Abeysekera, W., Hall, C., Spall, S. K., Wang, B., Xiong, Y. et al. (2015). TRAF2 regulates TNF and NF-kappaB signalling to suppress apoptosis and skin inflammation independently of Sphingosine kinase 1. *eLife* **4**, 27667.

Franco, C. A., Jones, M. L., Bernabeu, M. O., Geudens, I., Mathivet, T., Rosa, A., Lopes, F. M., Lima, A. P., Ragab, A., Collins, R. T. et al. (2015). Dynamic endothelial cell rearrangements drive developmental vessel regression. *PLoS Biol.* **13**, e1002125.

Franco, C. A., Jones, M. L., Bernabeu, M. O., Vion, A.-C., Barbacena, P., Fan, J., Mathivet, T., Fonseca, C. G., Ragab, A., Yamaguchi, T. P. et al. (2016). Non-canonical Wnt signalling modulates the endothelial shear stress flow sensor in vascular remodelling. *eLife* **5**, 1024.

Fuchs, Y. and Steller, H. (2011). Programmed cell death in animal development and disease. *Cell* **147**, 742-758.

Hahn, P., Lindsten, T., Ying, G.-S., Bennett, J., Milam, A. H., Thompson, C. B. and Dunaief, J. L. (2003). Proapoptotic bcl-2 family members, Bax and Bak, are essential for developmental photoreceptor apoptosis. *Invest. Ophthalmol. Vis. Sci.* **44**, 3598-3605.

Hahn, P., Lindsten, T., Tolentino, M., Thompson, C. B., Bennett, J. and Dunaief, J. L. (2005). Persistent fetal ocular vasculature in mice deficient in bax and bak. *Arch. Ophthalmol.* **123**, 797-802.

Hughes, S. and Chan-Ling, T. (2000). Roles of endothelial cell migration and apoptosis in vascular remodeling during development of the central nervous system. *Microcirculation* **7**, 317-333.

Ishida, S., Yamashiro, K., Usui, T., Kaji, Y., Ogura, Y., Hida, T., Honda, Y., Oguchi, Y. and Adamis, A. P. (2003). Leukocytes mediate retinal vascular remodeling during development and vaso-obliteration in disease. *Nat. Med.* **9**, 781-788.

Kisanuki, Y. Y., Hammer, R. E., Miyazaki, J.-i., Williams, S. C., Richardson, J. A. and Yanagisawa, M. (2001). Tie2-Cre transgenic mice: a new model for endothelial cell-lineage analysis in vivo. *Dev. Biol.* **230**, 230-242.

Kochhan, E., Lenard, A., Ellertsdottir, E., Herwig, L., Affolter, M., Belting, H.-G. and Siekmann, A. F. (2013). Blood flow changes coincide with cellular rearrangements during blood vessel pruning in zebrafish embryos. *PLoS ONE* **8**, e75060.

Koenig, M. N., Naik, E., Rohrbeck, L., Herold, M. J., Trounson, E., Bouillet, P., Thomas, T., Voss, A. K., Strasser, A. and Coultas, L. (2014). Pro-apoptotic BIM is an essential initiator of physiological endothelial cell death independent of regulation by FOXO3. *Cell Death Differ.* **21**, 1687-1695.

Korn, C. and Augustin, H. G. (2015). Mechanisms of vessel pruning and regression. *Dev. Cell* **34**, 5-17.

Korn, C., Scholz, B., Hu, J., Srivastava, K., Wojtarowicz, J., Arnsperger, T., Adams, R. H., Boutros, M., Augustin, H. G. and Augustin, I. (2014). Endothelial cell-derived non-canonical Wnt ligands control vascular pruning in angiogenesis. *Development* **141**, 1757-1766.

Kuipers, D., Mehonic, A., Kajita, M., Peter, L., Fujita, Y., Duke, T., Charras, G. and Gale, J. E. (2014). Epithelial repair is a two-stage process driven first by dying cells and then by their neighbours. *J. Cell Sci.* **127**, 1229-1241.

Kurihara, T., Kubota, Y., Ozawa, Y., Takubo, K., Noda, K., Simon, M. C., Johnson, R. S., Suematsu, M., Tsubota, K., Ishida, S. et al. (2010). von Hippel-Lindau protein regulates transition from the fetal to the adult circulatory system in retina. *Development* **137**, 1563-1571.

Lenard, A., Daetwyler, S., Betz, C., Ellertsdottir, E., Belting, H.-G., Huisken, J. and Affolter, M. (2015). Endothelial cell self-fusion during vascular pruning. *PLoS Biol.* **13**, e1002126.

Lindsten, T., Ross, A. J., King, A., Zong, W.-X., Rathmell, J. C., Shiels, H. A., Ulrich, E., Waymire, K. G., Mahar, P., Frauwirth, K. et al. (2000). The combined functions of proapoptotic Bcl-2 family members bak and bax are essential for normal development of multiple tissues. *Mol. Cell* **6**, 1389-1399.

Llambi, F., Moldoveanu, T., Tait, S. W. G., Bouchier-Hayes, L., Temirov, J., McCormick, L. L., Dillon, C. P. and Green, D. R. (2011). A unified model of mammalian BCL-2 protein family interactions at the mitochondria. *Mol. Cell* **44**, 517-531.

Lobov, I. B., Rao, S., Carroll, T. J., Vallance, J. E., Ito, M., Ondr, J. K., Kurup, S., Glass, D. A., Patel, M. S., Shu, W. et al. (2005). WNT7b mediates macrophage-induced programmed cell death in patterning of the vasculature. *Nature* **437**, 417-421.

Meeson, A., Palmer, M., Calfon, M. and Lang, R. (1996). A relationship between apoptosis and flow during programmed capillary regression is revealed by vital analysis. *Development* **122**, 3929-3938.

Mosinger Ogilvie, J., Deckwerth, T. L., Knudson, C. M. and Korsmeyer, S. J. (1998). Suppression of developmental retinal cell death but not of photoreceptor degeneration in Bax-deficient mice. *Invest. Ophthalmol. Vis. Sci.* **39**, 1713-1720.

Naik, E., O'Reilly, L. A., Asselin-Labat, M.-L., Merino, D., Lin, A., Cook, M., Coultas, L., Bouillet, P., Adams, J. M. and Strasser, A. (2011). Destruction of tumor vasculature and abated tumor growth upon VEGF blockade is driven by proapoptotic protein Bim in endothelial cells. *J. Exp. Med.* **208**, 1351-1358.

Potente, M., Gerhardt, H. and Carmeliet, P. (2011). Basic and therapeutic aspects of angiogenesis. *Cell* **146**, 873-887.

Pournaras, C. J., Rungger-Brändle, E., Riva, C. E., Hardarson, S. H. and Stefansson, E. (2008). Regulation of retinal blood flow in health and disease. *Prog. Retin. Eye Res.* **27**, 284-330.

Rao, S., Chun, C., Fan, J., Kofron, J. M., Yang, M. B., Hegde, R. S., Ferrara, N., Copenhagen, D. R. and Lang, R. A. (2013). A direct and melanopsin-dependent fetal light response regulates mouse eye development. *Nature* **494**, 243-246.

Saint-Geniez, M. and D'Amore, P. A. (2004). Development and pathology of the hyaloid, choroidal and retinal vasculature. *Int. J. Dev. Biol.* **48**, 1045-1058.

Savant, S., La Porta, S., Budnik, A., Busch, K., Hu, J., Tisch, N., Korn, C., Valls, A. F., Benest, A. V., Terhardt, D. et al. (2015). The orphan receptor Tie1 controls angiogenesis and vascular remodeling by differentially regulating Tie2 in tip and stalk cells. *Cell Rep.* **12**, 1761-1773.

Schindelin, J., Arganda-Carreras, I., Frise, E., Kaynig, V., Longair, M., Pietzsch, T., Preibisch, S., Rueden, C., Saalfeld, S., Schmid, B. et al. (2012). Fiji: an open-source platform for biological-image analysis. *Nat. Methods* **9**, 676-682.

Scholz, B., Korn, C., Wojtarowicz, J., Mogler, C., Augustin, I., Boutros, M., Niehrs, C. and Augustin, H. G. (2016). Endothelial RSPO3 controls vascular stability and pruning through non-canonical WNT/Ca(2+)/NFAT signaling. *Dev. Cell* **36**, 79-93.

Simonavicius, N., Ashenden, M., van Weverwijk, A., Lax, S., Huso, D. L., Buckley, C. D., Huijbers, I. J., Yarwood, H. and Isacke, C. M. (2012). Pericytes promote selective vessel regression to regulate vascular patterning. *Blood* **120**, 1516-1527.

Stahl, A., Connor, K. M., Sapieha, P., Chen, J., Dennison, R. J., Krah, N. M., Seaward, M. R., Willett, K. L., Aderman, C. M., Guerin, K. I. et al. (2010). The mouse retina as an angiogenesis model. *Invest. Ophthalmol. Vis. Sci.* **51**, 2813-2826.

Stalmans, I., Ng, Y.-S., Rohan, R., Fruttiger, M., Bouché, A., Ÿuce, A., Fujisawa, H., Hermans, B., Shani, M., Jansen, S. et al. (2002). Arteriolar and venular patterning in retinas of mice selectively expressing VEGF isoforms. *J. Clin. Invest.* **109**, 327-336.

Strasser, A., Jost, P. J. and Nagata, S. (2009). The many roles of FAS receptor signaling in the immune system. *Immunity* **30**, 180-192.

Vince, J. E. and Silke, J. (2016). The intersection of cell death and inflammasome activation. *Cell. Mol. Life Sci.* **73**, 2349-2367.

Wang, S., Park, S., Fei, P. and Sorenson, C. M. (2011). Bim is responsible for the inherent sensitivity of the developing retinal vasculature to hyperoxia. *Dev. Biol.* **349**, 296-309.

Watson, E. C., Whitehead, L., Adams, R. H., Dewson, G. and Coultas, L. (2016). Endothelial cell survival during angiogenesis requires the pro-survival protein MCL1. *Cell Death Differ.* **23**, 1371-1379.

Wei, M. C., Zong, W.-X., Cheng, E. H.-Y., Lindsten, T., Panoutsakopoulou, V., Ross, A. J., Roth, K. A., MacGregor, G. R., Thompson, C. B. and Korsmeyer, S. J. (2001). Proapoptotic BAX and BAK: a requisite gateway to mitochondrial dysfunction and death. *Science* **292**, 727-730.

Wilhelm, K., Happel, K., Eelen, G., Schoors, S., Oellerich, M. F., Lim, R., Zimmermann, B., Aspalter, I. M., Franco, C. A., Boettger, T. et al. (2016). FOXO1 couples metabolic activity and growth state in the vascular endothelium. *Nature* **529**, 216-220.

Xu, Q., Wang, Y., Dabdoub, A., Smallwood, P. M., Williams, J., Woods, C., Kelley, M. W., Jiang, L., Tasman, W., Zhang, K. et al. (2004). Vascular development in the retina and inner ear: control by Norrin and Frizzled-4, a high-affinity ligand-receptor pair. *Cell* **116**, 883-895.

Yu, D.-Y., Su, E.-N., Cringle, S. J., Morgan, W. H., McAllister, I. L. and Yu, P. K. (2016). Local modulation of retinal vein tone. *Invest. Ophthalmol. Vis. Sci.* **57**, 412-419.